scientific reports

Check for updates

OPEN

Functional changes of precuneus architecture across newborns, infants, and early adolescents

Jiaojian Wang[1,2], Qinmu Peng[1,2], Minhui Ouyang[1,2], Ruolin Li[1,3], Wentao Wu[1,3], Lu Zhang[1,4], Yun Peng[5] & Hao Huang[1,2]✉

Brain functional development from birth to adolescence follows the cortical gradient from primary sensorimotor to higher-order association regions. Precuneus (PCun) is crucial in spatial cognition, visual-motor integration, and social cognition. However, functional connectivity changes of PCun subregions in this dynamic developmental period are not known. Multimodal cross-sectional diffusion MRI and resting-state fMRI of subjects from birth to early adolescence were acquired to obtain structural and functional connectivity. PCun in neonates, 1-year-olds, 2-year-olds, and early adolescent subjects were consistently parcellated into four subregions based on structural connectivity of PCun. Significant developmental changes were found in functional connectivity between the parcellated PCun subregions and default mode network (DMN), and between the parcellated PCun subregions and cerebellum network. To understand altered development of PCun in brain disorders, connectivity-based parcellation was performed in the subjects with autism spectrum disorder (ASD). Similar parcellation pattern of PCun was found, but the relative volume of the dorsal-posterior subregion significantly decreased in the subjects with ASD compared to typically developmental subjects. These findings revealed functional developmental patterns of PCun subregions in their connected networks in typical developing brains and revealed PCun subregion alteration in ASD, shedding light onto functional changes of PCun architecture during development.

Keywords Precuneus, Structural connectivity, Parcellation, Typical development, Functional connectivity, Autism spectrum disorder

The brain development, especially from birth to early adolescence, plays a pivotal role in normal maturation of brain cognitive functions. Altered development leads to a diversity of neurodevelopmental disorders including autism spectrum disorder (ASD), attention-deficit hyperactivity disorder, and schizophrenia[1]. During this period, synaptic maturation and pruning[2], myelination[3,4], the appearance and disappearance of transient cellular compartments, cell types, and synaptic circuits[5] were observed, leading to the emergence of macroscopical neural connectivity of the brain[6]. Underlaid by dramatic structural and microstructural changes of the developmental human brain, the brain follows remarkable functional changes following the cortical development gradient[7] from primary sensorimotor, visual functions to higher order cognitive functions, such as attention, memory, language, social cognition, and executive control.

Precuneus (PCun), in the medial parietal cortex, has been widely reported to be involved in a wide range of primary and higher order functions including visuospatial imagery, episodic memory retrieval, self-processing, and consciousness[8–10]. The PCun and several other brain areas displayed the highest metabolic rates during the resting state while suppressed during externally focused and attention-demanding goal-directed tasks[11]. These brain areas exhibiting most active during the resting state constitute default mode network (DMN)[12]. PCun is demonstrated to be the posterior core hub of the DMN[13]. Furthermore, graph-theory based brain structural and functional network analyses revealed that PCun is also the hub of the whole brain in both adult and childhood for global information integration[14–16]. The functional centrality of this region corresponds to its marked evolutionary expansion in the hominin lineage[17], suggesting its potential role in supporting advanced cognitive

[1]Department of Radiology, Children's Hospital of Philadelphia, Philadelphia, PA 19104, USA. [2]Department of Radiology, Perelman School of Medicine, University of Pennsylvania, Philadelphia, PA 19104, USA. [3]Department of Bioengineering, University of Pennsylvania, Philadelphia, PA 19104, USA. [4]Graduate School of Education, Peking University, Beijing 100871, China. [5]Department of Radiology, Beijing Children's Hospital, Capital Medical University, Beijing 100045, China. ✉email: hao.huang@pennmedicine.upenn.edu

capacities unique to humans. Therefore, it is important to delineate the developmental functional organization of PCun at a fine-grained scale for understanding its crucial role in brain functional maturation.

The advances of magnetic resonance imaging techniques, especially diffusion magnetic resonance imaging (dMRI) and resting-state functional MRI (rs-fMRI), have played a critical role in delineating adult brain structural and functional connectivity, respectively. Two approaches based on dMRI have been used to parcellate the brain regions. The high contrasts of dMRI-derived maps can be directly used to parcellate adult and developmental human brain, mainly the white matter, to establish atlases[18–22]. It has been demonstrated that brain regions with no clear sulcal boundaries or contrast such as certain cortical gyrus, thalamus or mid-sagittal corpus callosum can also be parcellated based on their distal connectivity patterns[23–25]. Such parcellations are associated with regional functions, especially as the structural connectivity is the functional backbone of the brain[26]. Since brain areas distinguished by different structural connectivity patterns, connectivity-based parcellation approach has been proposed and applied to parcellate a brain area into subregions with each subregion characterized by unique functional specialization. Connectivity-based parcellations were consistent with the findings obtained from histological mapping such as cytoarchitecture and myeloarchitecture[27–29]. Significant structural[16,30–35] and functional[36] connectivity changes have been revealed in developmental brain in various stages from infancy to adolescence. By non-invasively mapping the structural connectivity in the developmental human brain cerebral cortex, cortical subregions without clear geometrical sulcal boundaries can be parcellated. These parcellated cortical subregions enable investigating the functional organization of the developmental brain at a fine-grained scale[33,37].

In this study, we aimed to reveal the typical developmental architecture and connectivity patterns of PCun through infancy and childhood and atypical functional organization of PCun in ASD using structural connectivity-based parcellation approach and resting-state functional connectivity (RSFC) analyses. The flowchart of the current study is demonstrated in Fig. 1. Specifically, structural connectivity-based parcellation was first used to parcellate the PCun to identify topographical organization in neonates, 1-year-old, 2-year-old, and early adolescent subjects. Subsequently, each of the PCun subregions was functionally characterized based on its RSFC patterns, and the functionally connected brain areas with PCun in early adolescent subjects were selected as target brain areas for the following functional connectivity mapping. Next, functional connectivity between PCun subregions and target brain areas were mapped and compared among neonates, 1-year-old, 2-year-old, and around puberty early adolescent subjects to reveal the typical developmental patterns. Finally, structural connectivity-based parcellation was applied to parcellate PCun in subjects with ASD to reveal the abnormal topographic organization.

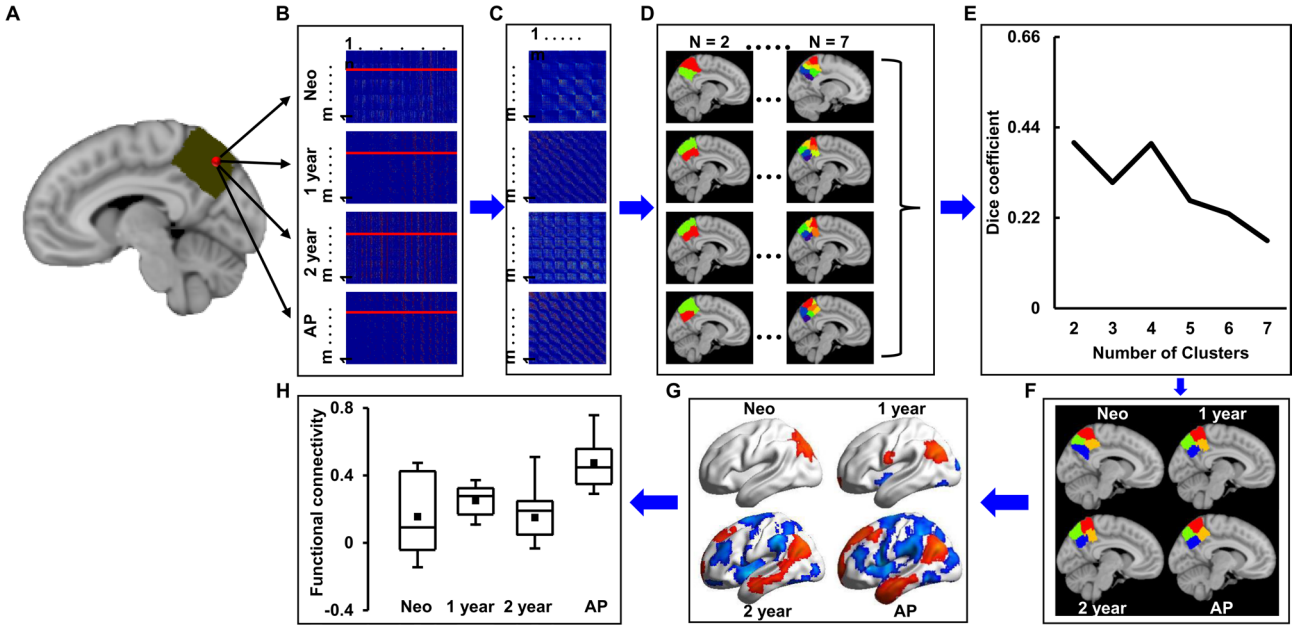

Fig. 1. Flowchart of this study. A, define the precuneus mask; B, calculate the whole brain anatomical connectivity matrix (m, rows correspond to each PCun voxel; n, columns correspond to each voxel of the whole brain); C, calculate the cross-correlation similarity matrix (m × m matrix, both rows and columns correspond to the number of voxels in the PCun seed mask); D, parcellate precuneus into 2–7 clusters; E, calculate the overlap degree with Dice coefficients between neonate (Neo), 1-year-old, 2-year-old, and around-puberty (AP) subjects; F, the optimal four-way parcellation of precuneus was determined; G, whole brain resting-state functional connectivity patterns for each precuneus subregion was mapped; H, quantify the developmental changes of functional connectivity with target brain areas for Neo 1-year-old, 2-year-old, and AP subjects.

Results

Parcellation of left and right PCun

Diffusion-MRI-based tractography was used to parcellate the left and right PCun, respectively. Dice coefficient identified the optimal 4 subregions in left and right PCun (Fig. 2A). For the left and right PCun, we found that the parcellation results are similar, with two subregions located in the dorsal PCun and two subregions located in the ventral PCun (Fig. 2B). The probability map for each PCun subregion was calculated and showed high probability of each subregion across the subjects (Fig. 2C). The individual parcellation results of left and right PCun for neonate, 1-year-old, 2-year-old, and early adolescent subjects can be found in Figure S1-S4, respectively.

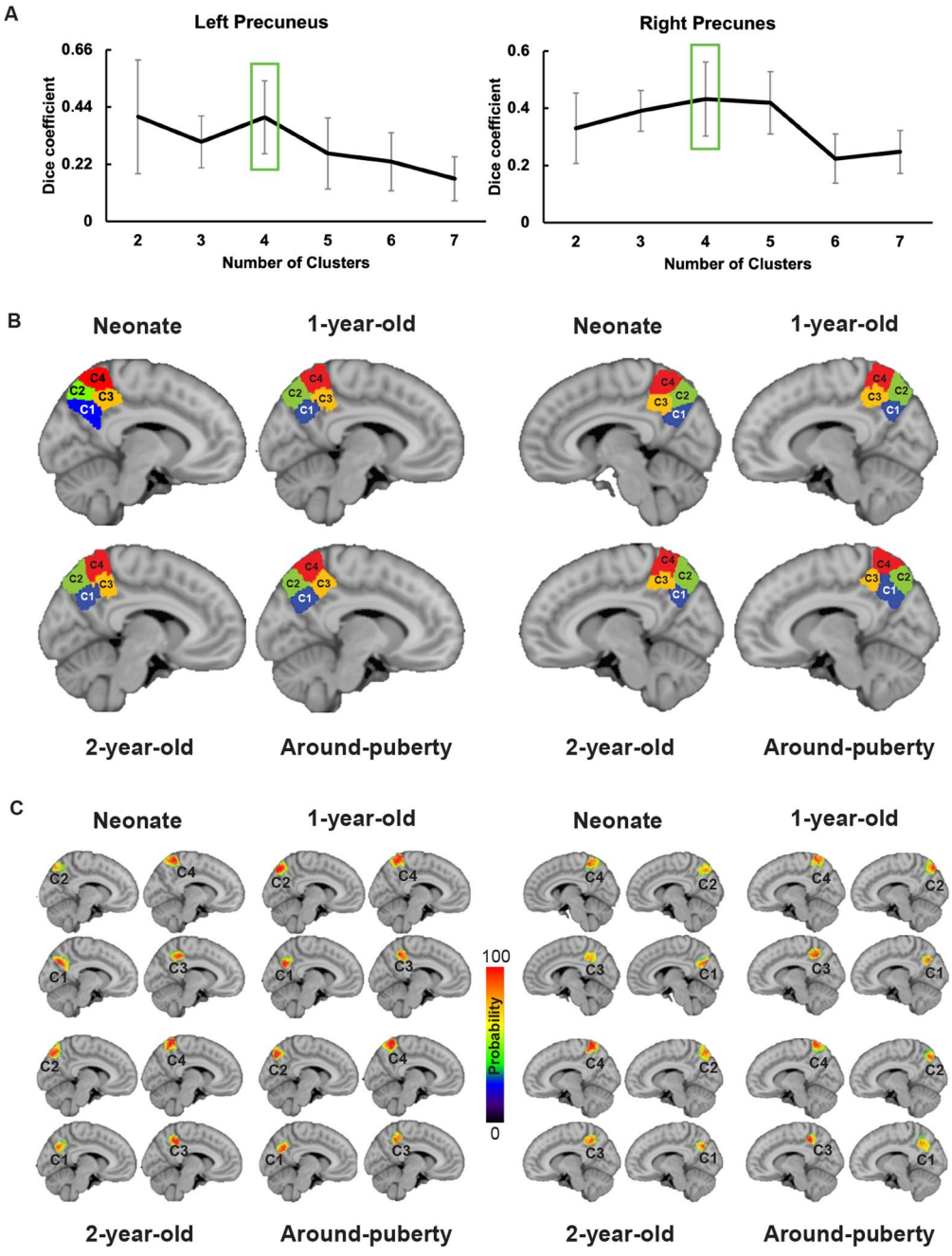

Fig. 2. Parcellation result for left and right precuneus (PCun). A, topographic similarity characterized using Dice coefficient across different groups (neonate, 1-year-old, 2-year-old, and around-puberty) was separately calculated for left and right PCun. The optimal four-way parcellation for left and right PCun was chosen for further analyses. B, group-population parcellation result of left and right PCun were created for neonate, 1-year-old, 2-year-old, and around-puberty subjects. C, the corresponding probability map of left and right PCun were calculated and shown for neonate, 1-year-old, 2-year-old, and around-puberty subjects.

We calculated the relative volume of each PCun subregion in neonate, 1-year-old, 2-year-old, and early adolescent subjects to determine the brain size changes during normal development. The relative volume showed that each PCun subregion has almost similar size across neonate, 1-year-old, 2-year-old, and around puberty subjects (Figure S5).

Resting-state functional connectivity patterns for PCun subregions

Whole brain functional connectivity pattern for each PCun subregion was mapped to identify the main cortical network that each subregion participates in (Fig. 3, FDR corrected; Figure S6, without thresholding). Whole brain functional connectivity mapping found that the primary positive functional connectivity in neonates are local connections with superior/inferior parietal lobule (S/IPL), whereas in 1-year-old, 2-year-old, and around-puberty subjects, the long-range functional connectivity was observed. Given that all the four subregions of PCun only have local connections in neonates (Fig. 3), thus, in the following paragraph, we only describe the functional connections to each PCun subregion in 1-year-old, 2-year-old, and around puberty subjects. In 1-year-old infants, left C1 mainly connects with ventral bilateral IPL, postcentral gyrus (PoCG), medial prefrontal cortex (MPFC), and medial temporal lobule (MTL), and right C1 shows main connections with bilateral IPL and MTL. In 2-year-old infants, left C1 connects with bilateral superior/middle frontal gyrus (S/MFG), middle temporal gyrus (MTG), MPFC and IPL, whereas right C1 functionally connects with bilateral IPL, MPFC, S/MFG, and right MTG. In around-puberty subjects, both left and right C1 primarily connect with bilateral S/MFG, IPL, MPFC, and MTG (Fig. 3). For C2, in 1-year-old infants, both left and right subregions functionally connect with bilateral IPL, S/IPL, and left posterior MTL, whereas right C2 also connects with right posterior MTL. In 2-year-old infants, both left and right C2 connect with bilateral dorsal premotor area (PMd), lateral orbital frontal cortex (LOFC), MTG, IPL, posterior MTL, MTG and right MFG. In around-puberty subjects, both left and right C2 show similar functional connectivity patterns with 2-year-old infants, but C2 in around-puberty subjects doesn't show functional connection with posterior MTL (Fig. 3). For C3, in 1-year-old infants, both left and right subregions show functional connections with bilateral MTL and IPL, whereas left C3 additionally connects to bilateral MPFC and right C3 shows additional connection with ventral postcentral gyrus (PoCG). In 2-year-old infants, left C3 connects with bilateral SFG, MPFC, IPL, MTL, MTG, caudate, and left LOFC; right C3 functionally connects with bilateral IPL, MPFC, caudate, MTL, and right MFG. In around puberty subjects, left C3 connects with bilateral IPL, MPFC, and MFG, and right C3 mainly connects with bilateral IPL and right MFG (Fig. 3). For C4, in 1-year-old infants, both left and right subregions connect with bilateral posterior MTL, posterior insula, paracentral lobule (PCL), and cingulate motor area (CMA); Left C4 additionally connects to lateral occipital cortex (LOC). In 2-year-old infants, left and right C4 connect with bilateral IPL, PCL, CMA, PMd, and right supramarginal gyrus (SMG); left C4 also connects with left MFG, and right C4 additionally connects to left LOC. In around puberty subjects, left and right C4 connect with bilateral PMd, LOC, thalamus, and PCL (Fig. 3).

Spatial correlation coefficients between the corrected functional connectivity patterns of each PCun subregion across neonates, 1-year-old, 2-year-old, and around puberty subjects were calculated to further delineate the whole brain functional connectivity pattern similarity. Spatial correlation analyses indicated an overall trend whereby functional connectivity patterns were more similar between temporally adjacent age groups, with similarity gradually decreasing as developmental distance increased (Figure S7).

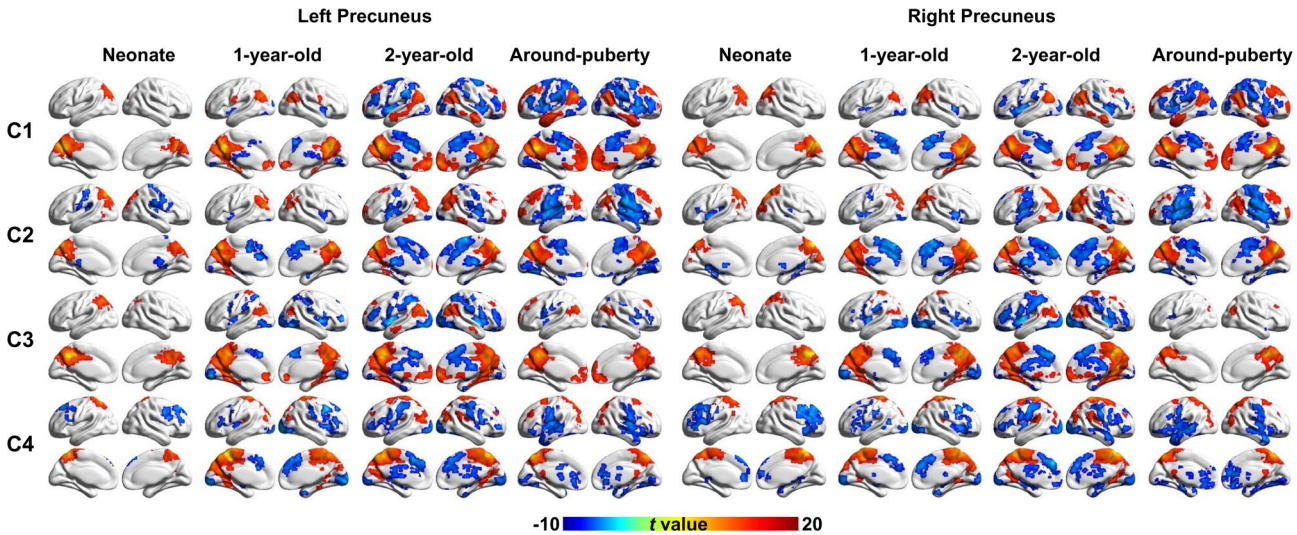

Fig. 3. Whole brain functional connectivity pattern for each PCun subregion. Whole brain functional connectivity pattern of each left and right precuneus subregion in neonate, 1-year-old, 2-year-old, and around-puberty subjects was mapped. The significant level was determined using false discovery rate (FDR) correction with $P < 0.05$ and minimum cluster size > 50.

Developmental patterns of functional connectivity

To characterize the developmental changes of functional connectivity for PCun, FCs between each PCun subregion and eleven target brain areas were calculated. The target brain areas include bilateral PMd, IPL, MFG, MTG, left MPFC, right LOFC, and cerebellum (Cereb) (Figure S8, peak coordinates in Table S1). The developmental changes of functional connections between PCun subregions and default mode network (DMN) and cerebellum network were identified (Fig. 4). No significant developmental changes in functional connections between PCun subregions and motor network were found (Figure S9).

Within DMN, we found developmental changes of functional connections between left C1and left IPL, MPFC (Fig. 4). For the functional connectivity between left C1 and left IPL, significantly increased functional connectivity were identified in 1-year-old, 2-year-old, and around puberty subjects compared to neonates; no significant differences in functional connectivity between left C1 and left IPL were identified between 1-year-old, 2-year-old, and around puberty subjects (Fig. 4). For the functional connectivity between left C1 and

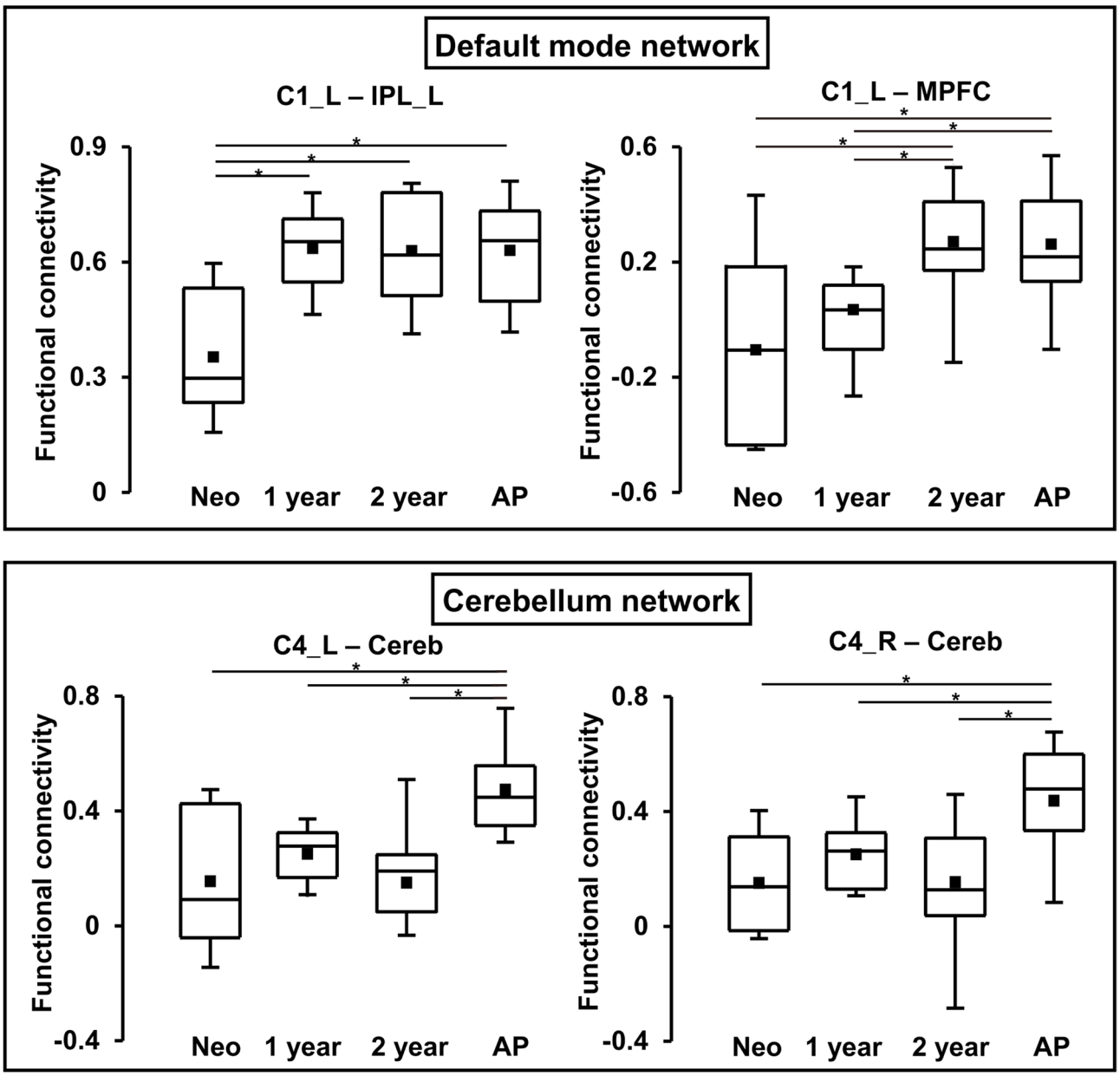

Fig. 4. Developmental changes of functional connectivity of precuneus (PCun). Functional connectivity analyses identified significant functional connectivity changes between PCun subregions and default mode network (DMN) and cerebellum network. Significant functional connectivity changes between left ventral posterior PCun subregion (C1) and left inferior parietal lobule (IPL_L), medial prefrontal cortex (MPFC) were found at 1-year-old and 2-year-old infants, respectively. Significantly increased functional connectivity between left and right dorsal anterior PCun subregion (C4) and cerebellum (Cereb) were found at 2-year-old infants. (Neo: neonate; AP: around-puberty; Only significant results are labeled in the figure.).

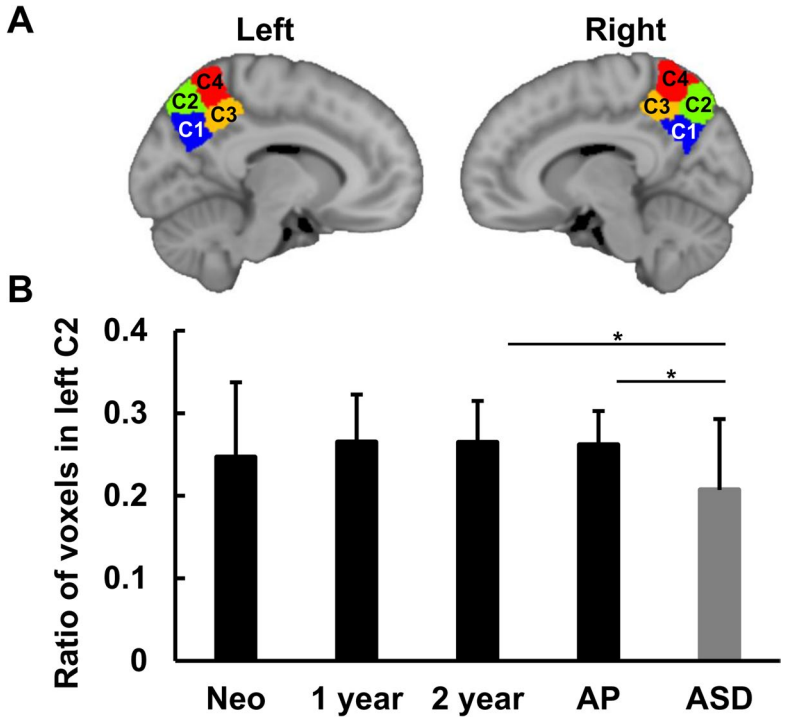

Fig. 5. Parcellation of precuneus (PCun) in autism spectrum disorder (ASD). (A) left and right PCun were parcellated into four subregions showing similar topographic patterns with typical development (TD) subjects. (B) to reveal the structural abnormality, comparisons of relative volume defined by the ratio of number of voxels of each PCun subregion divided by the total number of voxels of the whole PCun were performed between all TD groups (neonate (Neo), 1-year-old, 2-year-old, and around-puberty (AP)) and ASD for all the PCun subregions. Significantly decreased relative volume of the left dorsal posterior PCun subregion (C2) was identified in ASD compared to 2-year-old infants and AP subjects.

MPFC, significantly increased functional connectivity were identified in 2-year-old and around puberty subjects compared to neonates and 1-year-old subjects. No significant differences in functional connectivity between left C1 and MPFC were identified between 1-year-old subjects and neonates, and between 2-year-old subjects and around puberty subjects (Fig. 4).

For cerebellum network, we found developmental changes of functional connections between bilateral C4 and right cerebellum (Fig. 4). Significantly increased functional connectivity between bilateral C4 and right cerebellum was found in around-puberty subjects compared to neonates, 1-year-old, and 2-year-old subjects; no significant differences in functional connectivity between bilateral C4 and right cerebellum were identified between neonates, 1-year-old, and 2-year-old subjects (Fig. 4).

To determine the DMN-related subregion in PCun, the functional connections between each PCun subregion and MPFC were calculated. The functional connectivity analyses found that both left and right C1 have strongest functional connectivity strength with MPFC in neonates, 1-year-old, 2-year-old, and around puberty subjects suggesting that C1 is the posterior core hub of DMN (Figure S10).

Parcellation of PCun in children with ASD

To explore whether abnormal development results in altered parcellation scheme for PCun, anatomical connectivity-based parcellation of PCun was performed in 14 ASD subjects and identified similar functional topography in ASD (Fig. 5A) compared to typical developmental subjects. The individual parcellation results of left and right PCun for ASD were shown in Figure S11. Compared to typically developmental subjects, we found the decreased relative volume of the dorsal posterior subregion (C2) of left PCun in ASD subjects compared to 2-year-old and around puberty subjects (Fig. 5B).

Discussion

In this study, we delineated the human precuneus PCun development from birth to puberty using structural connectivity-based parcellation and resting-state functional connectivity mapping. Across 4 landmark cross-sectional ages, PCun exhibited a similar functional topographical organization. In neonates, the PCun showed primarily local functional connections, whereas by 1 year of age, long-range functional connections of PCun began to emerge. During development, significant changes in functional connectivity were observed between the PCun and DMN as well as between the PCun and the cerebellum network. Moreover, structural connectivity-based parcellation identified a similar functional topographic architecture of PCun in individuals with ASD, but the atypical development was characterized by a reduced relative volume of the posterior dorsal PCun

subregion in ASD compared to typical development individuals. Taken together, these findings demonstrate that combining structural connectivity-based parcellation with resting-state functional connectivity mapping provides important insights into both typical and atypical development of the PCun, shedding light on its crucial role in brain functional maturation.

Parcellation of PCun based on structural connectivity from infancy to puberty

Extensive studies have revealed significant structural[16,30–34,37] connectivity changes in developmental brain. After dramatic structural connectivity changes in fetal stage and postnatal stage before 1 year of age[35,38–43], the structural connectivity changes are much slower as demonstrated by the relatively stable PCun parcellation based on structural connectivity. Functional specification subregions of PCun in adult brain have been delineated in previous studies using cytoarchitecture[44], receptor distribution patterns[45], structural and functional connectivity-based parcellation mapping[46]. Critically, although different schemes exist, a central consensus is that the heterogeneous structural connectivity of the PCun underlies its functional segregation and determines its coupling with distinct large-scale resting-state networks[47]. However, whether and how this fundamental structure-function relationship is established during early brain development remains unclear. To address this gap, we applied a structural connectivity-based parcellation approach and identified a similar organization architecture of PCun across neonates, 1-year-old, 2-year-old, and around puberty subjects. Our parcellation scheme for PCun across the 4 groups is consistent with previous resting-state functional connectivity-based mapping of this area[48], suggesting functional topography is underpinned by structural connectivity patterns[10,28,49]. Crucially, the parcellation of the PCun identified in this study, based on structural connectivity, revealed a clear and consistent dorsal-ventral organizational architecture[56], with two subregions in the dorsal PCun and two subregions in the ventral PCun. The dorsal anterior PCun subregion (C4) showed primary functional connections with precentral, postcentral, and paracentral gyri, suggesting a role in sensorimotor processing[50]. The functional connectivity between C4 and prefrontal cortex is also observed suggesting its involvement in the preparation or execution of spatially guided behaviors[51]. The dorsal posterior PCun subregion (C2) mainly connected with the visual cortex, supporting functions in mental imagery[52,53]. Previous fMRI studies also demonstrated that the dorsal posterior PCun is a part of parietal memory network participating in episodic memory retrieval[8]. The ventral anterior PCun subregion (C3) showed strong connectivity with ventral medial prefrontal cortex and parahippocampus, indicating a potential role in limbic system for emotion processing[48]. The ventral posterior PCun subregion (C1), which aligned with the 'central precuneus' region described in the literature for its role in high-level cognitive integration[48,54], was primarily connected with DMN regions, indicating C1's role as a posterior DMN hub[15,55]. This finding was corroborated by functional connectivity analysis to MPFC in our study. Moreover, this stable PCun functional topography is supported by recent morphological evidence showing that the shape of this structure, as reflected by the proportion of the precuneus relative to overall brain length, is largely stable from birth, with its dorsal and ventral regions constituting distinct morphological modules[57]. The convergence between our stable parcellation patterns across different age groups and the early-established morphological modularity strongly indicates that the fundamental functional architecture of the PCun is already established at birth.

Developmental functional connectivity pattern between PCun and DMN

Resting-state functional connectivity mapping identified the posterior ventral PCun subregion (C1) as a posterior hub of DMN. Consistent with prior resting-state fMRI studies that DMN emerged at term-born neonates[14,58–60] and exhibited adult-like topology of by 1 year[61,62], we found that C1 showed mainly local connections in neonates, whereas the long-range connectivity of C1 with DMN emerged at 1 year and remained stable across 1-year-old, 2-year-old and early adolescent groups. Despite the similar DMN topology, different developmental patterns of functional connectivity strength between C1 and DMN subareas were identified. For example, C1-IPL functional connectivity increased significantly at 1 year old, whereas strong C1-MPFC functional connectivity strengthen was found in 2 years old, suggesting the differential maturation of functional connectivity within DMN regions. Such differential maturation of functional connectivity may reflect the functional segregation within DMN[13], in which precuneus, posterior cingulate cortex and MPFC serve as core hubs for self-relevant and affective decisions, and IPL as part of medial temporal subsystem engaged in memory-based scene construction[13], and also indicates that 1 and 2 years represent crucial developmental windows for these respective systems. Given that structural connectivity forms the backbone of functional connectivity, the differential maturation of functional connectivity within DMN regions likely reflects underlying white matter development. In early postnatal life, the short-range fibers are dominant and strengthen rapidly, while long-range fibers gradually mature over the first 2 years of life[32]. Since C1 connects to the IPL via short-range connections and to the MPFC via long-range connections, the distinct developmental windows for functional connectivity may reflect the dynamic developmental changes of short- and long-range structural connections[32]. Moreover, the differential maturation of DMN hubs during the first two years of life was supported by heterogeneous increases in regional cerebral blood flow across hub regions during this early stage[62,63]. Nevertheless, although we found significant functional connectivity changes in different periods, whether these changes directly underline emerging behavioral performances and cognitive functions needs to be further investigated.

Developmental functional connectivity pattern between PCun and the cerebellum network

Differential functional connectivity between the dorsal anterior PCun subregion (C4) and cerebellum was observed. While cerebellum is traditionally associated with motor execution, control, coordination and balance[64], a growing body of literature indicates its involvement in other cognitive functions, such as planning, working memory, set-shifting, abstract reasoning, emotion regulation, and visual-spatial organization[65]. In infant brain, the white matter fiber pathway between cerebellum and cortex has also been well delineated[19,20,35,38,66]. The

cerebellum volume undergoes a remarkable 240% increase in the first year of life[67] and continues to grow throughout childhood, eventually following an inverted U-shaped developmental trajectory that peaks at age 11.8 years in females and 15.6 years in males[68]. All these studies suggested ongoing developmental changes in cerebellum through birth to adolescence. Although the structural changes of cerebellum were observed, the functional development of cerebellum remains less understood. Using resting-state functional connectivity analyses, we found that connectivity between C4 and cerebellum is significantly stronger in early adolescent subjects compared to neonates, 1-year-old, and 2-year-old infants, with no significant differences detected among the three younger age groups. These findings suggest that functional development, particularly cortico-cerebellar connectivity, is protracted and structural maturation likely precedes functional changes in cerebellum during early development.

PCun in children with ASD

PCun in ASD demonstrated similar functional topography with typically developing individuals, but the relative volume of the left dorsal posterior PCun subregion (C2) is smaller compared to 2-year-old and early adolescent subjects. These structural abnormalities of dorsal posterior PCun in ASD were supported by previous fMRI studies. In children with ASD (ages 7–12 years), reduced functional connectivity was observed between the PCun and regions including cuneus, caudate and dorsal medial thalamic nuclei[69]. Decreased functional connectivity between dorsal posterior PCun and frontal cortex was also reported in adults with ASD[70]. Both studies revealed the hypoconnectivity of PCun in ASD. In contrast, younger children with ASD from 2 to 7 years of age showed hyperconnectivity of the PCun with middle frontal gyrus, which correlated with symptom severity[71], highlighting age-dependent alterations in PCun connectivity in ASD. In addition to connectivity abnormality, behavioral studies have reported episodic memory deficits in ASD[72], suggesting that difficulties in retrieving stored information may impair the ability to reconstruct past experiences or simulate possible future or fictitious events[73,74]. These findings suggest that PCun abnormalities in ASD are associated with impairments in episodic memory retrieval and mental imagination.

Limitations and future directions

This study has several limitations. First, while we revealed the early stability of the PCun's functional architecture, variation in the individual parcellation exists, consistent with previous studies reporting pronounced inter-individual variations in morphological and connectivity measures of PCun e.g.,[56,75,76]. Future studies with larger cohorts are needed to evaluate the generalizability of our findings and to investigate the effect of genetic and environmental factors on individual variation of PCun's structure and function. Second, we recognize the cross-sectional design of the current study with notable gaps between sampled ages. Future longitudinal studies are warranted to confirm these findings and to fully characterize continuous developmental trajectories of PCun. In addition, the early-stabilized dorsal-ventral modular architecture identified here provides a valuable developmental baseline for understanding PCun function in broader contexts. An important future direction is to investigate how this early-established architecture influences the region's function across the entire lifespan and confers differential susceptibility to various pathological states e.g.,[77,78]. We demonstrated the translational application of the precuneus parcellation by incorporating ASD cohort and revealing local alterations within the precuneus in this ASD cohort. Future studies including larger samples of ASD cohort, broader age ranges, and multimodal characterization will be necessary to enable an in-depth and comprehensive investigation of precuneus alterations in ASD. Integrating this developmental perspective with research on aging and neurodegeneration may also provide novel insights into the role of the precuneus across the lifespan.

In conclusion, we identified a consistent developmental functional topography of PCun in neonates, 1-year-old and 2-year-old infants, early adolescent and ASD subjects, indicating that the fundamental functional architecture of the human PCun is established around birth. Resting-state functional connectivity analysis revealed distinct developmental windows of functional connectivity within DMN and cortical-cerebellar networks. These findings shed light on understanding the developmental mechanism of PCun and its deficits in neurodevelopmental disorders.

Materials and methods

Subjects and MRI data acquisition

The diffusion-weighted images (DWI) of all subjects were visually inspected by one of the authors (J.W.). After exclusion of corrupted data due to subject motion of 3 neonates, high-quality diffusion magnetic resonance imaging (dMRI) and structural MRI data from 21 neonates (16 males/5 females; age range of 37.6–41.6 gestational weeks with mean and standard deviation of 39.8 ± 1.3 gestational weeks at scan), 18 1-year-old infants (12 males/6 females; age range of 8.5–15.2 months old with mean and standard deviation of 12.2 ± 2.3 months at scan), and 18 2-year-old infants (9 males/9 females; age range of 20–24.4 months old with mean and standard deviation of 21.6 ± 1.5 months at scan) were kept. To evaluate the maturity level of the PCun in the early childhood period, 17 around puberty subjects (10 males/7 females; age range of 9.4–14.8 years old with mean and standard deviation of 11 ± 3.1 years at scan) were also recruited. The neonate MRI data was acquired at Children's Medical Center at Dallas, affiliated to UT Southwestern Medical Center, and the 1-year-old, 2-year-old, and around-puberty subjects were acquired at Beijing Children's Hospital. The MRI data in both sites were scanned using Philips 3 T Achieva MR scanners. The imaging protocols were identical for data acquisition of all participated subjects. All neonates included were part of the cohort for studying normal perinatal and prenatal development and were selected after rigorous screening procedures conducted by an experienced neonatologist. Exclusion criteria include mother's excessive drug or alcohol abuse during pregnancy; grade III–IV intraventricular hemorrhage; periventricular leukomalacia; hypoxic–ischemic encephalopathy; lung disease or brochopulmonary dysplasia; necrotizing enterocolitis that requires intestinal resection or complex

feeding/nutritional disorders; defects or anomalies of the forebrain, brainstem, or cerebellum; brain tissue dys- or hypoplasias; abnormal meninges; alterations in the pial or ventricular surface; or WM lesions[16]. Neonates were well fed before scanning. All neonate scans were conducted during their natural sleep. Earplugs, earphones and foam padding were applied to reduce the sound of the scanner. dMRI data were acquired using a single shot echo planar imaging. The parameters for neonate dMRI scanning were: time echo (TE) = 78 ms, time repetition (TR) = 6850 ms, in-plane FOV = 168 × 168 mm^2, in-plane imaging resolution = 1.5 × 1.5 mm^2, slice thickness = 1.6 mm, no gap, 30 independent diffusion-weighted directions uniformly distributed in space, b-value = 1000 s/mm^2, 1 non-diffusion-weighted images (b = 0 s/mm^2), repetition = 2. With 30 DWI volumes and 2 repetitions, DWI volumes that were corrupted due to artifacts or motion were replaced by the good volumes of another DTI repetition during postprocessing[16]. All included 1-year-old and 2-year-old infants and around-puberty subjects were healthy subjects with normal neurological and psychological records. For 1-year-old and 2-year-old infants, scans were performed under sedation. For 1-year-old, 2-year-old, and around puberty subjects' dMRI data, the imaging parameters were: TR = 7731ms, TE = 82.8 ms, in-plane FOV = 224 × 224 mm^2, in-plane imaging resolution = 2 × 2 mm^2, slice thickness = 2 mm, 30 independent diffusion-weighted directions uniformly distributed in space with b-value = 1000 s/mm^2, 1 non-diffusion-weighted images (b = 0 s/mm^2), repetition = 2. T1-weighted magnetization-prepared rapid gradient-echo (MPRAGE) images (T1w) were acquired for 1-year-old, 2-year-old, and around puberty subjects. The imaging parameters for MPRAGE were: TR = 8.3 ms, TE = 3.7 ms, voxel size = 1 × 0.78 × 0.78 mm^3, FOV = 200 × 180 × 140 mm^3. The MPRAGE images provide superior gray and white matter contrast and were used for registration. Resting-state functional MRI (rs-fMRI) data for all the 4 groups were also acquired. For 11 of 21 neonates, the scanning parameters were: TR = 1500 ms, TE = 27 ms, FOV = 168 × 168 × 90 mm^3, axial slice thickness = 3 mm, with no gap, voxel size = 2.4 × 2.4 × 3 mm, 210 volumes. Rs-fMRI data for 9 of 18 1-year-old, 13 of 18 2-year-old, and 17 around puberty subjects were also acquired with the following parameters: TR = 2000 ms, TE = 24 ms, FOV = 220 × 220 × 147 mm^3, axial slice thickness = 3 mm, 1 mm gap, voxel size = 3.44 × 3.44 × 3 mm, 200 volumes. T1w, dMRI and rs-fMRI images were acquired in the same session.

To further investigate abnormal development pattern of PCun, 14 subjects with autism spectrum disorder (ASD) (all males; age range of 2.7–3.5 years old with mean and standard deviation of 3.1 ± 0.3 years at scan; all Asian) were also included. The dMRI data of the 14 subjects with ASD were obtained at Beijing Children's Hospital. Please refer to our previous publication[71] on ASD diagnosis criteria. The imaging parameters were the same as those used in scanning 1-year-old, 2-year-old, and around-puberty subjects. All experimental protocols involving human subjects were approved by the Institutional Review Board of the Children's Medical Center at Dallas and the Children's Hospital in Beijing. Parents or legal guardians of all minor participants provided informed written consent for participation. All methods were carried out in accordance with relevant guidelines and regulations, including the Declaration of Helsinki.

Definition of PCun

PCun seed mask was manually drawn on template images (Fig. 1A). In neonate, the PCun was drawn on a T2 weighted template[19]. For 1-year-old and 2-year-old, the PCun was drawn on an unpublished in-house structural T1 template of 2-year-old[20]. The PCun around puberty was drawn on a template of standard space (MNI152 structural template). Mask boundaries were defined as follows. The posterior boundary of PCun was the medial portion of the parieto-occipital fissure, and the anterior boundary was the marginal branch of the cingulate sulcus. The ventral boundary of PCun is defined by the subparietal sulcus which horizontally extended anteriorly to marginal branch of the cingulate sulcus and posteriorly to parieto-occipital fissure. Subsequently, the PCun masks were warped into the individual diffusion space for probabilistic tracking.

MRI data preprocessing

DMRI data for each subject was corrected for head motion and eddy current distortion by registering all DWIs to the b0 image using affine transformation with FSL software (http://www.fmrib.ox.ac.uk/fsl). Next, b0 image of each neonate was registered to a 37-week brain template[79] and an inverse transformation was performed to transform the seed masks of the left and right PCun into the diffusion space for each subject for fiber tracking. For 1-year-old, 2-year-old, and around puberty subjects, we first registered each subject T1 image to template images, and an inverse transformation was performed to transform the seed masks of the left and right PCun into individual T1 space. Then, each subject T1 image was registered to b0 image, and the transformation was applied to transform the seed masks of left and right PCun into the diffusion space for fiber tracking.

The resting-state fMRI data was preprocessed using SPM8 software and Data Processing Assistant for Resting-State fMRI (DPARSF: www.restfmri.net/forum/DPARSF). The preprocessing steps included the first 15 volumes were removed to facilitate magnetization equilibrium effects. The remaining functional data were then realigned to the first volume for head motion correction. The data was discarded if the head-movement exceeded one voxel in any direction, and under these criteria, no subject was excluded. The rs-fMRI images were normalized to a T2 template for neonates and the EPI template for 1-year-old, 2-year-old, and around puberty subjects and resampled to a 3 × 3 × 3 mm^3 voxel-size. Subsequently, the rs-fMRI data were smoothed with a Gaussian kernel of 6 mm full-width at half maximum (FWHM), and Friston's 24 head motion parameters, white matter, and cerebrospinal fluid signals were regressed out. Finally, the functional images were filtered with a temporal band-pass of 0.01–0.1 Hz. To further exclude the head motion effects on functional connectivity analysis, scrubbing method was conducted to censor each subject's rs-fMRI time series to find out the mean frame displacement (FD) > 0.5 mm, and one volume before and two volumes after the bad volume were discarded[80]. One neonate subject was discarded because the remaining time points were far below half of the total time points of rs-fMRI data. Same preprocessing procedures elaborated in our previous publication were used[62]. To map the whole brain functional connectivity patterns of each PCun subregion, the global signal was regressed during fMRI data

preprocessing. For seed-to-target functional connectivity analysis, the global signal was not regressed to exclude the effects of negative functional connectivity.

Parcellation of the PCun based on structural connectivity

Diffusion probabilistic tractography was performed for each voxel in the PCun mask using the FSL package. Probability distributions were estimated for two fiber directions at each voxel[80]. Probabilistic tractography was applied by sampling 5000 streamline fibers in each voxel in the seed region to estimate the connectivity probability. To facilitate data storage and analysis, all of the whole brain connectivity patterns for each voxel were down sampled to 5 mm isotropic voxels. The connectivity matrix consisted of rows (m) indicating each PCun voxel and columns (n)representing each voxel of the whole brain (Fig. 1B). From this connectivity matrix, a symmetric cross-correlation matrix was generated (Fig. 1C). The size of this cross-correlation matrix wasm × m, where m was the number of voxels in the PCun seed mask, and the (i, j) element value is the correlation between the connectivity profile of the PCun voxel *i* and the connectivity profile of the PCun voxel *j*[81].

The similarity matrix was then segmented using spectral clustering for automated clustering to define different numbers of clusters from 2 to 7[27,82]. Then, the maximum probability map was created for each solution across all the subjects. To calculate the maximum probability map, we transformed each individual parcellation result from the diffusion space to the MNI152 template in MNI space. The maximum probability map was calculated across all the subjects in each group by assigning each voxel of the reference space to the area in which it was most likely to be located. If two areas showed the same probability at a particular voxel, this voxel was assigned to the area with the higher average probabilities of the 26 voxels directly adjacent[27,82].

To determine the optimal number of clusters, the Dice coefficient was used. The number of clusters associated with maximum consistency of the population-level maximum probability maps across neonate, 1-year-old, 2-year-old, and around puberty groups was set as the optimal number of clusters. Based on the optimal parcellation, the relative volume defined as the ratio of number of voxels in each subregion divided by the total number of voxels within the whole PCun mask was calculated to quantify the size of each PCun subregion.

Resting-state functional connectivity analyses

To determine the whole brain RSFC patterns for each subregion, we first resampled the PCun subregions to 3 mm cubic voxels in MNI space. FC was defined by the Pearson correlation coefficients between the mean time series for each PCun subregion and the mean time series for each voxel of the whole brain. The correlation coefficient r value was converted to z values using Fisher' s z transformation to improve normality. Then each individual' s z-values were entered into a random effects one-sample t-test in a voxel-wise manner to determine the regions that showed significant correlations with the seed region. Finally, the functional connectivity map was thresholded using false discovery rate (FDR) correction method with $P < 0.05$ and cluster size > 50 voxels.

To characterize the developmental changes of functional connectivity for PCun, FCs between each PCun subregion and target brain areas were calculated. The target brain areas were defined from the functional connectivity patterns of PCun subregions in around-puberty subjects. To define the corresponding target brain areas, the whole brain functional connectivity pattern of each PCun subregion of around puberty subjects was corrected using FDR method as stated above, and the positively connected brain areas for each PCun subregion were used as the target brain areas. The peak coordinates of these positively connected target brain areas were obtained and used to draw spheres with 6 mm radium to calculate functional connections. FCs were computed through Pearson's correlations between the averaged time series of seed areas and corresponding target brain areas in neonates, 1-year-old, 2-year-old and around puberty subjects. Next, nonparametric Wilcoxon rank sum test, which is equivalent to the Mann-Whitney U test, was performed to determine the significant developmental changes in functional connectivity. The significant level was corrected using Bonferroni correction method with $P < 0.05$.

Spatial correction was also used to quantify the similarity of the whole brain functional connectivity patterns of each PCun subregion between neonates, 1-year-old, 2-year-old and around puberty subjects. To calculate the spatial correction, the statistical FC map for each PCun subregion obtained using one-sample t-test was thresholded using FDR method as stated above. Then, Pearson' s correlation coefficients were calculated between any pair of thresholded FC maps of neonates, 1-year-old, 2-year-old and around puberty subjects.

Moreover, to identify the default mode network (DMN) related subregion in PCun, functional connectivity between each PCun subregion and medial prefrontal cortex (MPFC) which is the anterior core hub of DMN[11] was calculated in neonates, 1-year-old, 2-year-old and around puberty subjects. The subregion showing strongest functional connectivity with MPFC was the posterior core hub of DMN.

Parcellation of PCun in ASD

To delineate atypical developmental topographic pattern of PCun, left and right PCun were also parcellated into the optimal number of clusters determined across neonate, 1-year-old, 2-year-old, and around-puberty subjects in ASD. The relative volume of each PCun subregion defined as a ratio of number of voxels in each subregion divided by the number of voxels of the whole PCun mask was calculated. Nonparametric Wilcoxon rank sum test was performed to identify whether the relative volume of each PCun subregion in ASD was different from the corresponding subregion in typical development subjects. The significant level was set at $P < 0.05$.

Data availability

All data required for reproducing our findings is available from the corresponding author upon reasonable request.

Received: 26 September 2025; Accepted: 16 February 2026

Published online: 26 February 2026

References

1. Marín, O. Developmental timing and critical windows for the treatment of psychiatric disorders. *Nat. Med.* **22**, 1229–1238. https://doi.org/10.1038/nm.4225 (2016).
2. Huttenlocher, P. R. & Dabholkar, A. S. Regional differences in synaptogenesis in human cerebral cortex. *J. Comp. Neurol.* **387**, 167–178. https://doi.org/10.1002/(sici)1096-9861(19971020)387:2%3C167::aid-cne1%3E3.0.co;2-z (1997).
3. Miller, D. J. et al. Prolonged myelination in human neocortical evolution. *Proc. Natl. Acad. Sci. USA* **109**, 16480–16485. https://doi.org/10.1073/pnas.1117943109 (2012).
4. Yakovlev, P. Regional Development of the Brain in Early Life. *Arch Dis Child*. **43**, 388–388. (1968).
5. Silbereis, J. C., Pochareddy, S., Zhu, Y., Li, M. & Sestan, N. The Cellular and Molecular Landscapes of the Developing Human Central Nervous System. *Neuron* **89**, 248–268. https://doi.org/10.1016/j.neuron.2015.12.008 (2016).
6. Tau, G. Z. & Peterson, B. S. Normal development of brain circuits. *Neuropsychopharmacol* **35**, 147–168. https://doi.org/10.1038/npp.2009.115 (2010).
7. Margulies, D. S. et al. Situating the default-mode network along a principal gradient of macroscale cortical organization. *Proc. Natl. Acad. Sci. USA* **113**, 12574–12579. https://doi.org/10.1073/pnas.1608282113 (2016).
8. Cavanna, A. E. & Trimble, M. R. The precuneus: a review of its functional anatomy and behavioural correlates. *Brain* **129**, 564–583. https://doi.org/10.1093/brain/awl004 (2006).
9. Dadario, N. B. & Sughrue, M. E. The functional role of the precuneus. *Brain* **146**, 3598–3607. https://doi.org/10.1093/brain/awad181 (2023).
10. Tanglay, O. et al. Anatomy and white-matter connections of the precuneus. *Brain Imaging Behav.* **16**, 574–586. https://doi.org/10.1007/s11682-021-00529-1 (2022).
11. Raichle, M. E. et al. A default mode of brain function. *Proc. Natl. Acad. Sci. USA* **98**, 676–682. https://doi.org/10.1073/pnas.98.2.676 (2001).
12. Buckner, R. L., Andrews-Hanna, J. R. & Schacter, D. L. The brain's default network: anatomy, function, and relevance to disease. *Annals New York Acad. Sciences* **1124**, 1–38. https://doi.org/10.1196/annals.1440.011 (2008).
13. Andrews-Hanna, J. R., Reidler, J. S., Sepulcre, J., Poulin, R. & Buckner, R. L. Functional-anatomic fractionation of the brain's default network. *Neuron* **65**, 550–562. https://doi.org/10.1016/j.neuron.2010.02.005 (2010).
14. Cao, M. et al. Early Development of Functional Network Segregation Revealed by Connectomic Analysis of the Preterm Human Brain. *Cereb Cortex* **27**, 1949–1963. https://doi.org/10.1093/cercor/bhw038 (2017).
15. Hagmann, P. et al. Mapping the structural core of human cerebral cortex. *PLoS biology* **6**, e159. https://doi.org/10.1371/journal.pbio.0060159 (2008).
16. Huang, H. et al. Development of human brain structural networks through infancy and childhood. *Cereb Cortex* **25**, 1389–1404. https://doi.org/10.1093/cercor/bht335 (2015).
17. Bruner, E., Preuss, T. M., Chen, X. & Rilling, J. K. Evidence for expansion of the precuneus in human evolution. *Brain Struct. Funct.* **222**, 1053–1060. https://doi.org/10.1007/s00429-015-1172-y (2017).
18. Oishi, K. et al. Multi-contrast human neonatal brain atlas: application to normal neonate development analysis. *Neuroimage* **56**, 8–20. https://doi.org/10.1016/j.neuroimage.2011.01.051 (2011).
19. Feng, L. et al. Age-specific gray and white matter DTI atlas for human brain at 33, 36 and 39 postmenstrual weeks. *Neuroimage* **185**, 685–698. https://doi.org/10.1016/j.neuroimage.2018.06.069 (2019).
20. Song, L. et al. Diffusion-tensor-imaging 1-year-old and 2-year-old infant brain atlases with comprehensive gray and white matter labels. *Human brain mapping* **45**, e26695. https://doi.org/10.1002/hbm.26695 (2024).
21. Mori, S. et al. Stereotaxic white matter atlas based on diffusion tensor imaging in an ICBM template. *Neuroimage* **40**, 570–582. https://doi.org/10.1016/j.neuroimage.2007.12.035 (2008).
22. Oishi, K., Chang, L. & Huang, H. Baby brain atlases. *Neuroimage* **185**, 865–880. https://doi.org/10.1016/j.neuroimage.2018.04.003 (2019).
23. Passingham, R. E., Stephan, K. E. & Kötter, R. The anatomical basis of functional localization in the cortex. *Nat. Rev. Neurosci.* **3**, 606–616. https://doi.org/10.1038/nrn893 (2002).
24. Behrens, T. E. et al. Non-invasive mapping of connections between human thalamus and cortex using diffusion imaging. *Nat. Neurosci.* **6**, 750–757. https://doi.org/10.1038/nn1075 (2003).
25. Huang, H. et al. DTI tractography based parcellation of white matter: application to the mid-sagittal morphology of corpus callosum. *Neuroimage* **26**, 195–205. https://doi.org/10.1016/j.neuroimage.2005.01.019 (2005).
26. van den Heuvel, M. P., Mandl, R. C., Kahn, R. S. & Hulshoff Pol, H. E. Functionally linked resting-state networks reflect the underlying structural connectivity architecture of the human brain. *Human brain mapping* **30**, 3127–3141. https://doi.org/10.1002/hbm.20737 (2009).
27. Wang, J. et al. Determination of the posterior boundary of Wernicke's area based on multimodal connectivity profiles. *Human brain mapping* **36**, 1908–1924. https://doi.org/10.1002/hbm.22745 (2015).
28. Wang, J. et al. Functional topography of the right inferior parietal lobule structured by anatomical connectivity profiles. *Human brain mapping* **37**, 4316–4332. https://doi.org/10.1002/hbm.23311 (2016).
29. Mars, R. B. et al. Diffusion-weighted imaging tractography-based parcellation of the human parietal cortex and comparison with human and macaque resting-state functional connectivity. *J. Neurosci.* **31**, 4087–4100. https://doi.org/10.1523/jneurosci.5102-10.2011 (2011).
30. Jeon, T., Mishra, V., Ouyang, M., Chen, M. & Huang, H. Synchronous Changes of Cortical Thickness and Corresponding White Matter Microstructure During Brain Development Accessed by Diffusion MRI Tractography from Parcellated Cortex. *Front. Neuroanat.* **9**, 158. https://doi.org/10.3389/fnana.2015.00158 (2015).
31. Lebel, C. & Beaulieu, C. Longitudinal development of human brain wiring continues from childhood into adulthood. *J. Neurosci.* **31**, 10937–10947. https://doi.org/10.1523/jneurosci.5302-10.2011 (2011).
32. Ouyang, M., Kang, H., Detre, J. A., Roberts, T. P. L. & Huang, H. Short-range connections in the developmental connectome during typical and atypical brain maturation. *Neurosci. Biobehav. Rev.* **83**, 109–122. https://doi.org/10.1016/j.neubiorev.2017.10.007 (2017).
33. Ouyang, M., Dubois, J., Yu, Q., Mukherjee, P. & Huang, H. Delineation of early brain development from fetuses to infants with diffusion MRI and beyond. *Neuroimage* **185**, 836–850. https://doi.org/10.1016/j.neuroimage.2018.04.017 (2019).
34. Yu, Q. et al. Microstructure, length, and connection of limbic tracts in normal human brain development. *Front. Aging Neurosci.* **6**, 228. https://doi.org/10.3389/fnagi.2014.00228 (2014).
35. Yu, Q. et al. Differential White Matter Maturation from Birth to 8 Years of Age. *Cereb Cortex* **30**, 2673–2689. https://doi.org/10.1093/cercor/bhz268 (2020).
36. Sanders, A. F. P. et al. Age-related differences in resting-state functional connectivity from childhood to adolescence. *Cereb Cortex* **33**, 6928–6942. https://doi.org/10.1093/cercor/bhad011 (2023).
37. Huang, H. Imaging the Infant Brain (*Oxford University Press*, (2022).
38. Huang, H. et al. White and gray matter development in human fetal, newborn and pediatric brains. *Neuroimage* **33**, 27–38. https://doi.org/10.1016/j.neuroimage.2006.06.009 (2006).

39. Huang, H. et al. Anatomical characterization of human fetal brain development with diffusion tensor magnetic resonance imaging. *J. Neurosci.* **29**, 4263–4273. https://doi.org/10.1523/jneurosci.2769-08.2009 (2009).
40. Ouyang, A. et al. Spatial mapping of structural and connectional imaging data for the developing human brain with diffusion tensor imaging. *Methods (San Diego, Calif)* **73**, 27–37. https://doi.org/10.1016/j.ymeth.2014.10.025 (2015).
41. Dubois, J. et al. Asynchrony of the early maturation of white matter bundles in healthy infants: quantitative landmarks revealed noninvasively by diffusion tensor imaging. *Human brain mapping* **29**, 14–27. https://doi.org/10.1002/hbm.20363 (2008).
42. Dubois, J. et al. Exploring the Early Organization and Maturation of Linguistic Pathways in the Human Infant Brain. *Cereb Cortex* **26**, 2283–2298. https://doi.org/10.1093/cercor/bhv082 (2016).
43. Huang, H. Structure of the fetal brain: what we are learning from diffusion tensor imaging. *Neuroscientist* **16**, 634–649. https://doi.org/10.1177/1073858409356711 (2010).
44. Scheperjans, F. et al. Observer-independent cytoarchitectonic mapping of the human superior parietal cortex. *Cereb Cortex* **18**, 846–867. https://doi.org/10.1093/cercor/bhm116 (2008).
45. Scheperjans, F., Palomero-Gallagher, N., Grefkes, C., Schleicher, A. & Zilles, K. Transmitter receptors reveal segregation of cortical areas in the human superior parietal cortex: relations to visual and somatosensory regions. *Neuroimage* **28**, 362–379. https://doi.org/10.1016/j.neuroimage.2005.06.028 (2005).
46. Zhang, Y. et al. Connectivity-based parcellation of the human posteromedial cortex. *Cereb Cortex* **24**, 719–727. https://doi.org/10.1093/cercor/bhs353 (2014).
47. Yamaguchi, A. & Jitsuishi, T. Structural connectivity of the precuneus and its relation to resting-state networks. *Neuroscience research* **209**, 9–17. https://doi.org/10.1016/j.neures.2023.12.004 (2024).
48. Margulies, D. S. et al. Precuneus shares intrinsic functional architecture in humans and monkeys. *Proc. Natl. Acad. Sci. USA* **106**, 20069–20074. https://doi.org/10.1073/pnas.0905314106 (2009).
49. Wang, J. et al. Convergent functional architecture of the superior parietal lobule unraveled with multimodal neuroimaging approaches. *Human brain mapping* **36**, 238–257. https://doi.org/10.1002/hbm.22626 (2015).
50. Herbet, G., Lemaitre, A-L., Moritz-Gasser, S., Cochereau, J. & Duffau, H. The antero-dorsal precuneal cortex supports specific aspects of bodily awareness. *Brain* **142**, 2207–2214. https://doi.org/10.1093/brain/awz179 (2019).
51. Wenderoth, N., Debaere, F., Sunaert, S. & Swinnen, S. P. The role of anterior cingulate cortex and precuneus in the coordination of motor behaviour. *Eur. J. Neurosci.* **22**, 235–246. https://doi.org/10.1111/j.1460-9568.2005.04176.x (2005).
52. Hanakawa, T. et al. Functional properties of brain areas associated with motor execution and imagery. *J. Neurophysiol.* **89**, 989–1002. https://doi.org/10.1152/jn.00132.2002 (2003).
53. Freton, M. et al. The eye of the self: precuneus volume and visual perspective during autobiographical memory retrieval. *Brain Struct. Funct.* **219**, 959–968. https://doi.org/10.1007/s00429-013-0546-2 (2014).
54. Yeager, B. E. et al. Central precuneus lesions are associated with impaired executive function. *Brain Struct. Funct.* **227**, 3099–3108. https://doi.org/10.1007/s00429-022-02556-0 (2022).
55. Fransson, P. & Marrelec, G. The precuneus/posterior cingulate cortex plays a pivotal role in the default mode network: Evidence from a partial correlation network analysis. *Neuroimage* **42**, 1178–1184. https://doi.org/10.1016/j.neuroimage.2008.05.059 (2008).
56. Jiang, P. et al. The hierarchical organization of the precuneus captured by functional gradients. *Brain Struct. Funct.* **228**, 1561–1572. https://doi.org/10.1007/s00429-023-02672-5 (2023).
57. Bruner, E. & Gallareto-Sande, R. Growth and development of the precuneus in humans from birth to early adulthood. *Cereb Cortex* **35**, bhaf305. https://doi.org/10.1093/cercor/bhaf305 (2025).
58. Fransson, P. et al. Resting-state networks in the infant brain. *Proc. Natl. Acad. Sci. USA* **104**, 15531–15536. https://doi.org/10.1073/pnas.0704380104 (2007).
59. Doria, V. et al. Emergence of resting state networks in the preterm human brain. *Proc. Natl. Acad. Sci. USA* **107**, 20015–20020. https://doi.org/10.1073/pnas.1007921107 (2010).
60. Smyser, C. D. et al. Longitudinal analysis of neural network development in preterm infants. *Cereb Cortex* **20**, 2852–2862. https://doi.org/10.1093/cercor/bhq035 (2010).
61. Gao, W. et al. Functional Network Development During the First Year: Relative Sequence and Socioeconomic Correlations. *Cereb Cortex* **25**, 2919–2928. https://doi.org/10.1093/cercor/bhu088 (2015).
62. Yu, Q. et al. Infant brain regional cerebral blood flow increases supporting emergence of the default-mode network. *Elife* **12**, e78397. https://doi.org/10.7554/eLife.78397 (2023).
63. Ouyang, M. et al. Spatiotemporal cerebral blood flow dynamics underlies emergence of the limbic-sensorimotor-association cortical gradient in human infancy. *Nat. Commun.* **15**, 8944. https://doi.org/10.1038/s41467-024-53354-7 (2024).
64. Evarts, E. V. & Thach, W. T. Motor mechanisms of the CNS: cerebrocerebellar interrelations. *Annu. Rev. Physiol.* **31**, 451–498. https://doi.org/10.1146/annurev.ph.31.030169.002315 (1969).
65. Buckner, R. L. The cerebellum and cognitive function: 25 years of insight from anatomy and neuroimaging. *Neuron* **80**, 807–815. https://doi.org/10.1016/j.neuron.2013.10.044 (2013).
66. Pieterman, K. et al. Cerebello-cerebral connectivity in the developing brain. *Brain Struct. Funct.* **222**, 1625–1634. https://doi.org/10.1007/s00429-016-1296-8 (2017).
67. Knickmeyer, R. C. et al. A structural MRI study of human brain development from birth to 2 years. *J. Neurosci.* **28**, 12176–12182. https://doi.org/10.1523/jneurosci.3479-08.2008 (2008).
68. Tiemeier, H. et al. Cerebellum development during childhood and adolescence: a longitudinal morphometric MRI study. *Neuroimage* **49**, 63–70. https://doi.org/10.1016/j.neuroimage.2009.08.016 (2010).
69. Lynch, C. J. et al. Default mode network in childhood autism: posteromedial cortex heterogeneity and relationship with social deficits. *Biological psychiatry* **74**, 212–219. https://doi.org/10.1016/j.biopsych.2012.12.013 (2013).
70. Salmi, J. et al. The brains of high functioning autistic individuals do not synchronize with those of others. *Neuroimage Clin.* **3**, 489–497. https://doi.org/10.1016/j.nicl.2013.10.011 (2013).
71. Ouyang, M. et al. Flattened Structural Network Changes and Association of Hyperconnectivity With Symptom Severity in 2-7-Year-Old Children With Autism. *Front. Neurosci.* **15**, 757838. https://doi.org/10.3389/fnins.2021.757838 (2021).
72. Crane, L. & Goddard, L. Episodic and semantic autobiographical memory in adults with autism spectrum disorders. *Journal autism Dev. disorders* **38**, 498–506. https://doi.org/10.1007/s10803-007-0420-2 (2008).
73. Lind, S. E. & Bowler, D. M. Episodic memory and episodic future thinking in adults with autism. *Journal Abnorm. psychology* **119**, 896–905. https://doi.org/10.1037/a0020631 (2010).
74. Li, W. et al. Disentangling the Switching Behavior in Functional Connectivity Dynamics in Autism Spectrum Disorder: Insights from Developmental Cohort Analysis and Molecular-Cellular Associations. *Adv. Sci.* **12**, e2403801. https://doi.org/10.1002/advs.202403801 (2025).
75. Bruner, E., Pereira-Pedro, A. S., Chen, X. & Rilling, J. K. Precuneus proportions and cortical folding: A morphometric evaluation on a racially diverse human sample. *Ann. Anat.* **211**, 120–128. https://doi.org/10.1016/j.aanat.2017.02.003 (2017).
76. Bruner, E., Román, F. J., de la Cuétara, J. M., Martin-Loeches, M. & Colom, R. Cortical surface area and cortical thickness in the precuneus of adult humans. *Neuroscience* **286**, 345–352. https://doi.org/10.1016/j.neuroscience.2014.11.063 (2015).
77. Bruner, E. et al. Morphological variations and cortical atrophy of the precuneus in normal aging and Alzheimer's disease. J. Anat. **248**, 62–70. https://doi.org/10.1111/joa.70027 (2026).
78. Tomasi, D. & Volkow, N. D. Aging and functional brain networks. Mol. Psychiatry **17**, 471, 549–558. https://doi.org/10.1038/mp.2011.81 (2012).

79. Serag, A. et al. Construction of a consistent high-definition spatio-temporal atlas of the developing brain using adaptive kernel regression. *Neuroimage* **59**, 2255–2265. https://doi.org/10.1016/j.neuroimage.2011.09.062 (2012).
80. Behrens, T. E., Berg, H. J., Jbabdi, S., Rushworth, M. F. & Woolrich, M. W. Probabilistic diffusion tractography with multiple fibre orientations: What can we gain? *Neuroimage* **34**, 144–155. https://doi.org/10.1016/j.neuroimage.2006.09.018 (2007).
81. Johansen-Berg, H. et al. Changes in connectivity profiles define functionally distinct regions in human medial frontal cortex. *Proc. Natl. Acad. Sci. USA* **101**, 13335–13340. https://doi.org/10.1073/pnas.0403743101 (2004).
82. Wang, J. et al. Tractography-based parcellation of the human left inferior parietal lobule. *Neuroimage* **63**, 641–652. https://doi.org/10.1016/j.neuroimage.2012.07.045 (2012).

Author contributions
H.H. and J.W. designed the research. J.W., Q.P., M.O., R.L., L.Z., Y.P. and H.H. performed the research. J.W., Q.P., and H.H. contributed new methodology and analytic tools. M.O. and H.H. supervised the collection of neuroimaging data. J.W. analyzed data, and generated figures and tables. J.W. wrote the original draft and all authors (J.W., Q.P., M.O., R.L., W.W., L.Z., Y.P. and H.H.) reviewed and revised the final draft.

Funding
This work was supported by grants from National Institute of Health: R01MH092535, R01MH125333, R01EB031284, R01MH129981, R21MH123930 and P50HD105354.

Declarations

Competing interests
The authors declare no competing interests.

Ethics declarations
Parents of all healthy and autism spectrum disorder subjects gave informed written consent approved by the Institutional Review Board of the Children's Medical Center at Dallas and the Children's Hospital in Beijing.

Additional information
Supplementary Information The online version contains supplementary material available at https://doi.org/10.1038/s41598-026-40813-y.

Correspondence and requests for materials should be addressed to H.H.